

Enhanced Optical Gap in Bi-layered Manganites $\text{La}_{2-2x}\text{Sr}_{1+2x}\text{Mn}_2\text{O}_7$ near $x = 0.4$ Myung W. Kim¹, H. J. Lee¹, B. J. Yang², Kee Hoon Kim², Y. Morimoto³, Jaejun Yu², and T. W. Noh^{1*}¹ReCOE & School of Physics, Seoul National University, Seoul 151-747, Korea²CSMR & School of Physics, Seoul National University, Seoul 151-747, Korea³Department of Physics, University of Tsukuba, Tsukuba 305-8573, Japan

We have systematically investigated the optical conductivity spectra of $\text{La}_{2-2x}\text{Sr}_{1+2x}\text{Mn}_2\text{O}_7$ ($0.3 \leq x \leq 0.5$). We find that just above the magnetic ordering temperatures, the optical gap shows an enhancement up to 0.3 eV near $x = 0.4$. Based on a x -dependent comparison of the nesting vector of the hypothetical Fermi surface and the superlattice wave-vector, we suggest that the peculiar x -dependence of the optical gap can be understood in terms of charge and lattice correlation enhanced by the charge density wave instability in nested Fermi surface.

PACS numbers: 75.47.Gk, 71.45.Lr, 74.25.Gz

The striped charge and spin correlation mark one of the generic features of doped Mott insulators with strong electron correlation. In particular, there exist numerous examples of the enhanced charge/spin correlation at commensurate hole doping, often signaled by an increased charge gap and anomalies in the spin/lattice degree of freedom. The famous $y = 1/8$ anomaly and stripe correlation in $\text{La}_{1-y}\text{Nd}_{0.4}\text{Sr}_y\text{CuO}_4$ [1], the static charge-spin stripe and an enhanced optical gap near $y = 1/3$ of $\text{La}_{2-y}\text{Sr}_y\text{NiO}_4$ [2, 3], and the CE-type charge/orbital order with a large optical gap near $y = 1/2$ of $\text{La}_{1-y}\text{Ca}_y\text{MnO}_3$ [4], all constitute well-known cases of the unusual stability of charge/spin correlation at the commensurate dopant levels. Although the anomalies at the specific commensurate dopant concentrations are fascinating in their own right, they are still not well understood. Furthermore, dynamic and/or short-ranged striped correlations remain as quite challenging issues in strongly correlated electron systems. They often exhibit themselves as an intriguing coexistence and coupling among charge/spin/lattice correlation at nanoscopic length scales.

$\text{La}_{2-2x}\text{Sr}_{1+2x}\text{Mn}_2\text{O}_7$ has exhibited an intriguing coexistence of striped charge/lattice correlations near or above the long range magnetic ordering temperature [5, 6]. From the early stages of the development of this field, the origin of the strong localization tendency of the doped holes has been a subject of continual interest and debates [7]. While the system is supposed to be a ferromagnetic (FM) metal at low temperatures, high resistivity [8] and non-Fermi type optical conductivity spectra [9] indicate that it should be close to a localized state. A recent angle-resolved photoemission (ARPES) experiment reported that a minimal Fermi surface (FS) of $x = 0.4$ is formed below T_C along the nodal direction while most of the 2D FS is gapped [10]. [Note that this anisotropic FS is quite similar to that of high T_C superconductors.] While strong electron-phonon interaction has been hypothesized to be a source of the localization, it is not clear how such a bosonic interaction microscopically influences a polaronic metal system with

an anisotropic band structure to tune localized states.

Herein, we report experimental findings on the enhanced optical gap in $\text{La}_{2-2x}\text{Sr}_{1+2x}\text{Mn}_2\text{O}_7$ (LSMO) near $x = 0.4$ through systematic doping dependent studies of optical conductivity spectra. The enhancement of the optical gap occurs at unusual specific hole doping, i.e. at $x = 0.4$, which is clearly distinguished in the previous well-known cases. Based on the comparison between the doping-dependent nesting vector of the FS and k -vector of the superlattice coming from the charge/lattice correlation, we suggest that charge density wave (CDW) instability in the nested FS plays a key role in causing the enhancement of the optical gap near $x = 0.4$.

Single crystals of $\text{La}_{2-2x}\text{Sr}_{1+2x}\text{Mn}_2\text{O}_7$ ($0.3 \leq x \leq 0.5$) were grown by the coating-zone method. The samples were characterized by resistivity and magnetization measurements [8]. For optical reflectivity measurements, cleaved ab-planes were prepared. Temperature (T) dependent reflectivity spectra $R(\omega)$ (ω is the photon energy) were measured at a temperature range of 15–300 K and over a wide ω range of 5 meV–30 eV. The NIM-Beam line at Pohang Accelerator Lab was used for the high energy (5–30 eV) measurement. We used the Kramers-Kronig transformation to obtain the optical conductivity spectra ($\sigma(\omega)$) from $R(\omega)$. Details of the optical experiments were described in a previous paper [9].

LSMO shows different magnetic ground states at different x [11]. For $x \leq 0.3$, the spins in the MnO_2 bilayers show FM alignment along the c -axis. For $0.33 \leq x \leq 0.4$, the FM spins align parallel to the ab -plane. For $0.4 \leq x \leq 0.5$, the alignment between MnO_2 layers becomes canted. Finally, A -type antiferromagnetic (AFM) order is stabilized for $x \geq 0.5$. We note that in all the compounds with $0.3 \leq x \leq 0.5$, the spins within a single MnO_2 layer are always ferromagnetically aligned below T_C or T_N , regardless of their long-range ordering pattern.

In Fig. 1 (a), $\sigma(\omega)$ of both $x = 0.45$ and 0.50 at $T = 15$ K are clearly suppressed below 1.0 eV, forming a finite optical gap. It is known that charge ordering (CO) instability occurs in $x = 0.50$ below 210 K, although it becomes unstable and short-ranged below 100 K with the

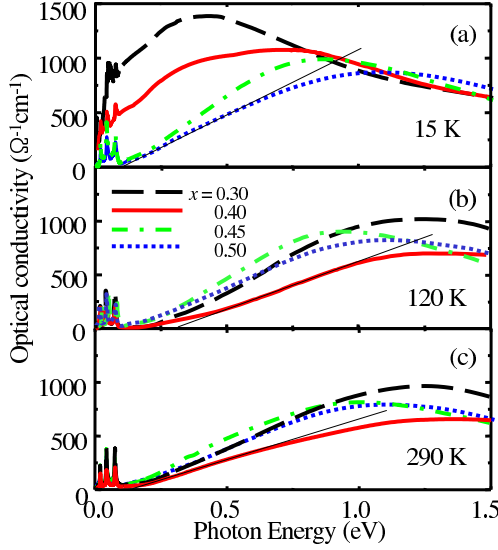


FIG. 1: (color online). (a) Optical conductivity $\sigma_1(\omega)$ of $\text{La}_{2-2x}\text{Sn}_{1+2x}\text{Mn}_2\text{O}_7$ ($0.3 \leq x \leq 0.5$) (a) at 15 K, (b) at 120 K, and (c) at 290 K. The thin solid lines represent the extrapolation for σ_2 estimate.

development of the A-type AFM state [12]. Therefore, the spectral features are consistent with the localization of carriers in short-ranged CO states for both compounds. We can define an optical gap (σ_2) as an onset energy of the steeply rising part of $\sigma_1(\omega)$ determined from a crossing point between the x abscissa and a linear extrapolation line drawn at the inflection point of $\sigma_1(\omega)$ (thin solid lines in Fig. 1), following the common practice used to evaluate σ_2 of various CO materials [4].

On the other hand, $\sigma_1(\omega)$ of $x = 0.30$ and 0.40 with the FM metallic ground state show broad maxima around 0.5 and 0.7 eV, respectively. The broad maximum, unexpected within the conventional D model, is the absorption due to the incoherent hopping motion of carriers from Mn^{3+} to Mn^{4+} sites [9, 13]. It is interesting that the existence of the $\sigma_1(\omega)$ maximum is accompanied by a decreasing σ_2 with $x \rightarrow 0$, resembling a gap feature observed in $x = 0.50$. We can attribute the decreasing behavior of σ_2 to the signature of the pseudo-gap even in the metallic states. Furthermore, the overall spectral shape in Fig. 1(a) suggests that the nature of the pseudo-gap might be directly related to the optical gap found in the $\sigma_1(\omega)$ of $x = 0.50$ and 0.45 at $T = 15$ K.

In Fig. 1(b), $\sigma_1(\omega)$ at 120 K reveal yet another intriguing finding. σ_2 (~ 0.3 eV) is clearly enhanced at the specific compound $x = 0.40$. It is even larger than that of $x = 0.50$ at which the CO state is stabilized. Such an enhanced σ_2 for $x = 0.40$ seems to exist even up to 290 K, as shown in Fig. 1(c). The x -dependent spectral response above T_C is counterintuitive because the σ_2 of $x = 0.40$ with a metallic ground state is clearly larger than that of $x = 0.50$ with the CO insulating state.

To understand the unexpected x -dependence of σ_2 at

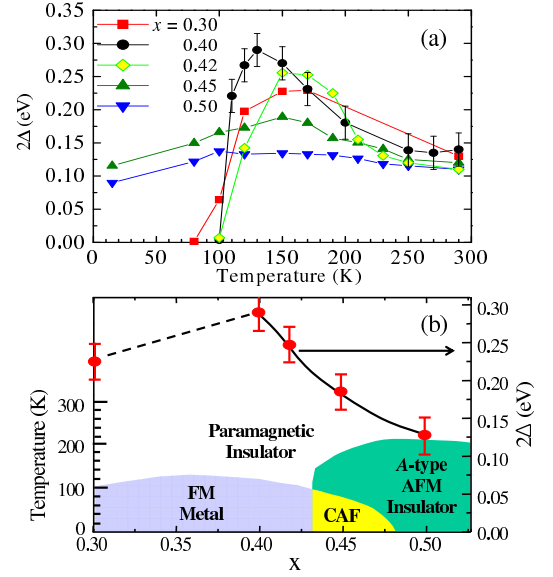


FIG. 2: (color online). (a) Temperature dependent σ_2 obtained from the $\sigma_1(\omega)$. The error bars of other compounds are almost the same size as that of $x = 0.40$. (b) x -dependence of σ_2 obtained at just above T_C or T_N is overlaid on the phase diagram. The lines are guides to the eyes.

120 K, we have systematically investigated T -dependence of σ_2 for all the samples. As shown in Fig. 2(a), T dependence of σ_2 confirms its anomalous enhancement near $x = 0.40$. First, σ_2 of both $x = 0.45$ and 0.50 compounds is only about 0.1 eV, and show a weak T -dependence. Furthermore, σ_2 of $x = 0.50$ even slightly decreases below 100 K in contrast to one of its 3D analogues [14]. On the other hand, in the compounds with $x = 0.30; 0.40$; and 0.42 , in which the 3D FM metallic ground states are stabilized, the σ_2 above T_C is larger than that of $x = 0.45$ or 0.50 . As displayed in Fig. 2(b), σ_2 values at just above T_C or T_N systematically increase from 0.1 (for $x = 0.50$) and 0.3 (for $x = 0.40$), and then decrease again to 0.2 eV (for $x = 0.30$).

The σ_2 value of $x = 0.50$ shows a decreasing behavior as T drops below around 100 K, as shown in Fig. 2(a). It is consistent with a previous neutron scattering experiment, which suggested the melting of CO correlation below 100 K with the stabilization of the 2D FM state [12]. Therefore, it is likely that CO correlation is rather weak at overall T in $x = 0.45$ and 0.50 , consistent with the weak or decreasing σ_2 behaviors shown in Fig. 2(a). On the other hand, the enhanced σ_2 near $x = 0.40$ above T_C gives rise to a surprising observation that the localization tendency could be at its largest for $x = 0.40$ just above its T_C while the system has a FM metallic ground state consistent with the collapse of σ_2 below T_C .

The enhancement of σ_2 above T_C in $x = 0.40$ is reminiscent of the similar behavior of σ_2 observed in other 3D manganite systems, i.e.: $\text{La}_{1-y}\text{Ca}_y\text{MnO}_3$ near $y = 0.50$: σ_2 at $T = 10$ K systematically increases from 0.1 to 0.5

eV as y decreases from 0.80 to 0.50. The enhancement of the CO gap at $y = 0.50$ is due to the unusual stability of the CE-type CO configuration at the commensurate doping. The finite Δ up to far above T_{CO} has been attributed to the short range, and the CE-type CO correlation resulting from the suppression of T_{CO} near a thermodynamic bi-critical point at $y = 0.50$ [4].

However, the finite and enhanced Δ behaviors above T_C in LSMO near $x = 0.40$ cannot be simply understood as a result of the proximity to the bi-critical point. As inferred from the phase diagram in Fig. 2(b), the possible bi-critical point, if any, should be rather close to $x = 0.45$; however, Δ of $x = 0.45$ shows much weaker T -dependence than that of $x = 0.40$. In addition, CO stability seems to be weak in the present system at overall x . The CO at the commensurate doping of $x = 0.50$ appears in a narrow T -range ($100 \text{ K} < T < 210 \text{ K}$), and even diminishes below 100 K with the AFM ordering [12]. Therefore, we argue that the origin of the enhanced Δ near $x = 0.40$ should be attributed to a new mechanism beyond the CE-type CO correlation.

A recent ARPES experiment has provided compelling evidence that FS of $x = 0.40$ is formed below T_C only along nodal direction while most of the 2D FS is gapped [10]. The resultant FS is highly nested with the nesting vector $q_F \approx 0.3$, which is susceptible to CDW formation, as suggested by Chuang et al [15]. The possibility of the CDW in $x = 0.40$ has been corroborated by x-ray scattering experiments [5, 6]; the stripe-like superlattice modulation vector $q_L \approx 0.3$ matches with the q_F [15].

The T -dependent Δ of the $x = 0.40$ in Fig. 2(a) is also consistent with CDW formation. Under CDW instability, the square of Δ develops in proportional to the superlattice peak intensity, I , that results from the periodic lattice modulation [16]. Strikingly, we found a close overlap between the square-root of I for the $(0.3;0;1)$ peak, observed by x-ray scattering experiments [5, 6] and the optical gap: i.e., $\Delta \propto \sqrt{I}$, as demonstrated in Fig. 3(a). Therefore, our optical study strongly suggests the formation of CDW instability in the $x = 0.40$.

Why, then, is CDW instability enhanced near $x = 0.40$? With the lack of x -dependent experimental FS data, we have theoretically investigated the FS topology of a MnO_2 layer. We used a tight-binding method, under the assumption that the local Mn spins are ferromagnetically aligned in a MnO_2 plane and e_g orbitals are doubly degenerate. Figs. 4(a) and 4(b) show the calculated FS, and Fig. 4(d) shows x -dependence of q_F from $x = 0.01$ to 0.5. In Fig. 4(c) we present the FS of $x = 0.40$, when spins are not polarized. The calculations reveal a couple of important findings: (1) The spin ordering is essential for the formation of the nested FS (Compare Fig. 4(b) with 4(c)). (2) The predicted q_F decreases from 0.50 (for $x = 0.01$) to 0.25 (for $x = 0.5$), with $q_F \approx 0.33$ for $x = 0.40$ being consistent with ARPES results [10, 15].

In contrast to the decreasing q_F in Fig. 4(d), the ex-

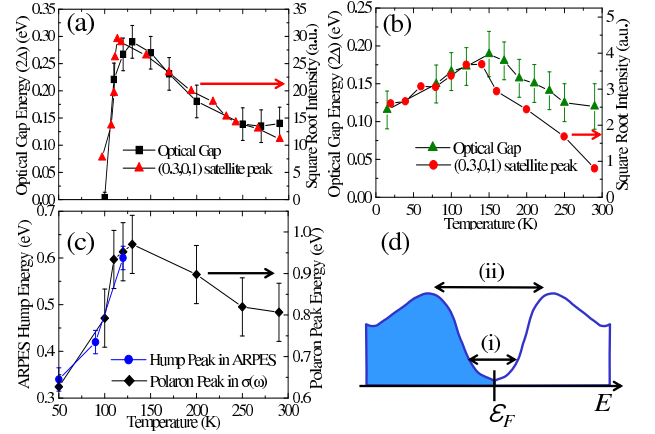


FIG. 3: (color online). Comparison between Δ and \sqrt{I} of $(0.3;0;1)$ superlattice peak (a) for $x = 0.40$ and (b) for $x = 0.45$. \sqrt{I} values were obtained from Ref. [5]. (c) Comparison between the hump peak energy in the ARPES spectra (Ref. [10]) and the incoherent absorption peak energy as determined by Lorentz oscillator fittings. (d) Schematic band diagram near the Fermi energy (E_F): (i) the pseudo-gap and (ii) the incoherent absorption (polaron) peak energy.

perimentally available points of q_L slowly increase as x increases in $0.3 < x < 0.5$, obtained from x-ray scattering experiments [5, 17]. It should be noted that in Fig. 4(d) the x -dependent q_F and q_L curves cross near $x = 0.40$. When x deviates from 0.40, the discrepancy between q_F and q_L actually increases, which suggests a scenario in which CDW instability could be mostly stabilized near $x = 0.40$ because of the close matching condition of q_F and q_L . Furthermore, in contrast to a simple 1D CDW case, q_F and q_L seem decoupled in this 2D system, suggesting that the coincident matching of the two vectors near $x = 0.40$ could have driven the stabilization of the CDW correlation due to the formation of the nested FS.

The CDW for other x , if formed, should be weaker than that of $x = 0.40$. This seems to be indeed consistent with the decreasing Δ behavior in Fig. 2(b) as x deviates from 0.40. Furthermore, the comparison between Δ of $x = 0.45$ and \sqrt{I} of the superlattice peak of $x = 0.44$ suggests that they are a better match with each other near T_C and below, as shown in Fig. 3(b). This finding supports the calculations in Fig. 4 that CDW stability can be achieved near $x = 0.40$ under FM spin ordering.

It is still an enigma why q_L slowly increases with x . The quasi-linear x dependence of q_L reminds us of a simple $q_L = x$ rule, which is experimentally found in the layered nickelates, which show striped CO correlation [1, 3]. The stripe-like lattice/charge correlation above T_C in this layered system can be a generic feature of doped Mott insulators due to the presence of strong Coulomb repulsion [1, 3]. Then, our present results suggest an appealing scenario in which the charge/lattice correlation synergistically complements the CDW correlation driven by the

